

SEISMIC STABILITY OF EMBEDDED TANK

By Takahiro Iwatate^I, Takeji Kokusho^I and Satoshi Ooaku^{II}

Summary

Shaking table tests have been performed to clarify the dynamic behaviors of embedded tanks in soft ground due to strong earthquake motions. Special care has been taken for the design of a soil container in order to reproduce ideal horizontal shear wave propagation in the model ground. Observed nonlinear responses of the embedded tanks due to various random motions are compared with the numerical results obtained from the axi-symmetric FEM analysis with equivalent linear method. This comparative study reveals that the proposed numerical analysis gives a useful key to estimate the dynamic behaviors of embedded tanks during strong earthquakes.

Scaled Model Vibration Tests

(1) The Model Ground A new type of a soil container has been developed in this research to reproduce the ideal horizontal shear motion in the model ground that excludes side wall constraints effects to the soil. Its walls consist of 16 rectangular steel hollow frames with 60 mm square cross-sectional area. These frames are set up one by one to form the side walls of one meter height with ball bearings at each contacting layer to ensure frictionless horizontal movements. The both side of all the walls are covered by the rubber membrane to make the box watertight. Special care was taken to reduce the weight of the wall to 9 to 12 percent of the contained soil. The fine clean sand was chosen as the material for the model ground which was dropped by the specially designed apparatus. It was a shallow box mounted on soil container whose bottom consists of twenty-four separate thin flaps rotating at the same moment when the lever is pulled. Such high void ratio as 0.87 was attained by this apparatus for the dry ground.

(2) The Model Tanks Three different model tanks which dimensions and material properties are presented in Table 1, were selected in order to experimentally simulate the dynamic motions of flexible and rigid tanks embedded in soft ground. These tanks, named here as A-Tank, B-Tank and C-Tank, have the same diameters and heights except for their thicknesses. The ratio of flexural rigity of A-Tank, B-Tank and C-Tank was 1:2:12.

Strain-gage type accelerometers (capacity 2G) were used to measure the vibrations of the tank and the ground at five different levels with approximate intervals of 25 cm. Five strain-gage type earthpressure gages (0.6 cm in diameter, 2 kg/cm² of capacity) were set on the wall surface of the tank to measure the dynamic earthpressures acted on the tank, and

I Senior Research Engineer, Central Research Institute of Electric Power Industry, Japan

II Kasumigaseki Information Center, Nikkagiken Corporation, Japan

strain gages were used to measure the dynamic strains of the tank. Small seismometers were set in the ground at four different levels for seismic explorations.

(3) Vibration Tests These vibration tests have been performed as follows.

(3-1) Seismic Exploration Tests and Free Vibration Tests The dynamic material properties of the model ground of both linear and non-linear were decided by the seismic explorations and the damped free oscillations of the model ground in its lowest natural frequency.

(3-2) Sinusoidal Vibrations Tests These tests were carried out under two different shaking table motions. (a) The sinusoidal vibration with constant base acceleration and alternating frequency. In this case, about five different base acceleration from 10 gal to 100 gal were selected as the constant base acceleration, and the frequency was changed smoothly from 5 Hz to 30 Hz with approximate increment of 0.5 Hz. (b) The sinusoidal vibration with the constant frequency and alternating amplitude of base acceleration. In the case, about five frequencies including the resonant one of the model, were selected and the base acceleration was increased gradually from 10 gal to 400 gal.

(3-3) Random Vibration Tests Two different random motions were selected to be applied to the model ground, which are named here as Ea and Ha. Ea was produced from El-Centro motion (1940, NS), while Ha from Hachinohe motion (1968), by appropriate time shortening processes. Ea motion has a rather flat spectrum of 8 to 22 Hz, whereas Ha motion has a high concentration of spectrum around 25 Hz. Ea and Ha motions were applied to the model tank with various magnitudes from 10 gal to 400 gal.

(4) Test Results

(4-1) Dynamic Material Properties of The Model Ground (a) The variation of shear moduli of the model ground determined by seismic explorations is shown in the logarithmic graph to be approximately proportional to square root of effective vertical stress, σ_v . (b) Material properties extracted from the damped free vibration of model ground of the model itself are shown in Fig. 4-1. They represent the average value of the model ground as a single degree of freedom system. The maximum shear modulus, G_{max} , derived in this way is equal to 74 kg/cm². (c) In order to extrapolate the G vs shear strain, γ curve and damping, h vs γ curve for larger strain range than the one experimentally determined, the theoretical model for strain-dependency of soil properties proposed by Hardin Drnevich (1970, b) was employed with some modifications. Using this modified model, G vs γ and h vs γ relations were obtained and shown in Fig. 4-1.

The details of dynamic properties of the model ground are to be referred to Ref. 3.

(4-2) Dynamic Responses of The Model Tanks (a) The resonance curves and acceleration responses of A-Tank, and model ground are shown in Fig. 4-2 and Fig. 4-3, respectively. The resonant frequency of 15.76 Hz

was observed with base acceleration of 10 gal. Comparing the dynamic motions of the tank with the ground motion, acceleration amplitudes and vibration modes coincide well with each other. The model tank moves in shearing mode predominantly at the resonant frequency. In the case of flexible tank, the difference in acceleration amplitude and phase lag between the tank and the surrounding ground was not observed clearly even at the large base acceleration ranges. While in the case of rigid tank (C-Tank), the differences in acceleration amplitude and the phase lag between the two were observed more remarkably with the increase of the base acceleration. (b) In Fig. 4-4, the ratios of the maximum accelerations of the ground and B-Tank to that of the base, are plotted against the maximum base acceleration for E_a and H_a motions respectively. The decrease in amplifications of the ground along with the magnitude increase of base acceleration is obviously seen. Thus the nonlinear properties of the ground have strong effects on the embedded tank. (c) Fig. 4-5 shows the observed maximum dynamic earthpressure distributions of B-Tank and C-Tank subjected to E_a and H_a motions. It is evidently seen that the remarkable difference exist in the distributions. In the case of flexible model (B-Tank), the earthpressure near the surface increases remarkably with the increase of the base acceleration, while in the case of rigid model (C-Tank) predominant earthpressure exists at around the bottom and its distributions look alike that of the hydrodynamic pressure. From the test results, it can be said that the ratio between the stiffness of the tank and that of the surrounding ground, have strong effects on the earthpressure distributions of the tanks. And the nonlinear properties of the model ground have strong effects on the dynamic earthpressures of the tank.

Complex Response Analysis of Embedded Tank

In order to analytically clarify the dynamic behaviors of embedded tanks during earthquake considering the nonlinear properties of the ground, a computer program for a complex response analysis of axi-symmetric soil-structure system combined with the equivalent linear method, has been developed.

According to this method, an approximate nonlinear solution can be obtained by linear analysis provided the stiffness and damping used in the analysis are compatible with the effective shear strain γ_{eff} , which is defined as the 65 percent of γ_{max} as is most widely used in engineering practice today.

Above mentioned analysis was applied to the scaled model vibration tests. The tank and surrounding ground were idealized by thin cylindrical shell element and by axi-symmetric solid element respectively.

(1) Numerical Results

(a) The first analysis is the dynamic linear analysis of A-Tank subjected to sinusoidal motions with base acceleration with 10 gal. The material properties of the tank presented in Table 1 were adopted. While the model ground was assumed to have the uniform single value of density γ' , shear modulus and damping ratio of $\gamma=1.42 \text{ g/cm}^3$, $G=74 \text{ kg/cm}^2$ and $h=0.05$. The calculated results were compared with experimental results and those

obtained from the conventional modal method. Fig. 6-1 shows the longitudinal distributions of maximum radial acceleration (RAcc), and maximum hoop stress (σ_{θ}) at the section of $\theta=0^{\circ}$. Analytical results obtained from these two methods well coincide each other.

(b) The second analysis is the dynamic nonlinear analysis of B-Tank subjected to both sinusoidal and two different random motions (E_a and H_a). For nonlinear analysis G vs γ , and h vs γ relations which are shown in Fig. 4-1 were adopted. Fig. 6-2 shows the longitudinal distribution of the maximum radial accelerations of the tank with base accelerations of 40 gal at 13 Hz, and 100 gal at 16 Hz, respectively. By comparing the results shown in Fig. 6-1 and one in Fig. 6-2 it is clearly seen that nonlinearity of the tank behavior is existing in the case of B-Tank and the analytical results also exhibits its nonlinear tendency. Fig. 6-3 shows the acceleration time histories at the surface due to the E_a motion with the base acceleration of 30 gal, and H_a motion with that of 50 gal, respectively. This figure shows that there exist some discrepancy between the experimental results and the analytical one, but agreements are fairly well between the two in large acceleration range which is most important from the engineering view points. Similar results are also obtained in the case of C-Tank.

Application to Actual L.N.G. Tank

The above mentioned analysis was also applied to actual L.N.G. concrete Tank embedded in the alluvial ground of which dimension and material properties were shown in Fig. 7-1. In this case input motion was taken from El-Centro motion (1940, NS) whose maximum acceleration was adjusted to 0.10 G.

The radial stresses of both linear and equivalent linear analysis are shown in Fig. 7-2 for the purpose of comparison. From the illustration, it can be concluded the introduction of linear effect is indispensable for reasonable estimation of those structure system, as expected.

Conclusive Remarks

The combined study of the scaled model vibration tests and numerical analysis has drawn a conclusion that the presented numerical analysis gives a reasonably well estimation of the dynamic behaviors of axi-symmetric soil structure system during strong earthquake.

The nonlinear properties of the model ground have strong effects on the acceleration responses and the dynamic earthpressures of the tanks.

References

- (1) Hardin, B.O. and Drnevich, V.P. (1970, b) "Shear modulus and Damping in Soil II. Design Equations and Curves", Technical Report, Soil Mechanics Series No. 2, University of Kentucky.
- (2) Iwatate, T., Kokusho, T. and Ooaku, S. "Seismic Stability of Embedded Tank" Proc. of 5th JEES, 1978 at Tokyo (in Japanese).
- (3) Kokusho, T., Iwatate, T. and Ooaku, S. "Scaled Model Tests and Numerical Analyses on Nonlinear Dynamic Response of Soft Grounds" Proc. of 5th JEES, 1978 at Tokyo.

Table 1 Dimension and Material Property of Model Tank

	A-Tank	B-Tank	C-Tank
Diameter	30cm	30cm	30cm
Height	100cm	100cm	100cm
Thickness	0.5mm	1.0mm	3.2mm
Material	Brass	Brass	Steel
Young's Modulus	kg/cm ² 1060000	kg/cm ² 1060000	kg/cm ² 2100000
Ratio of Flexural Rigidity	1	2	12

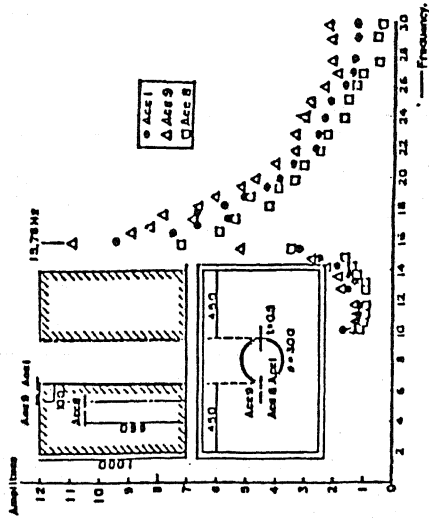


Fig. 4-2 Resonance Curves of A-Tank

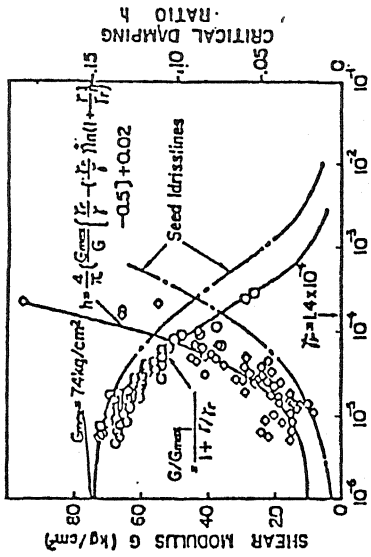


Fig. 4-1 Strain-Dependency of Shear Modulus and Damping

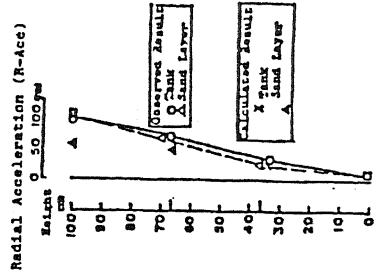


Fig. 4-3 Dynamic Motion of A-Tank at Resonant Frequency of 16 Hz

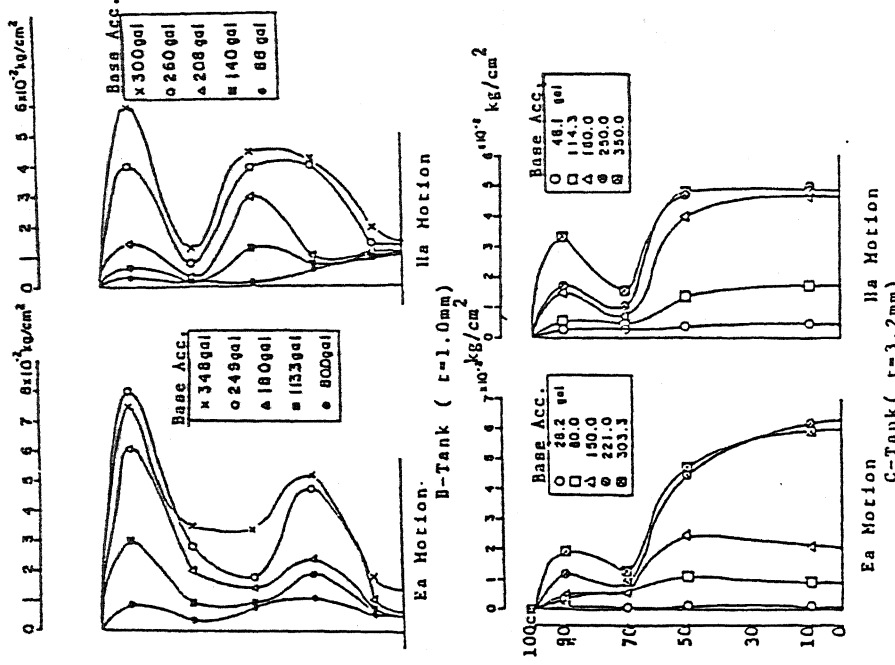


Fig. 4-5 Dynamic Earthpressure Distributions of Model Tanks

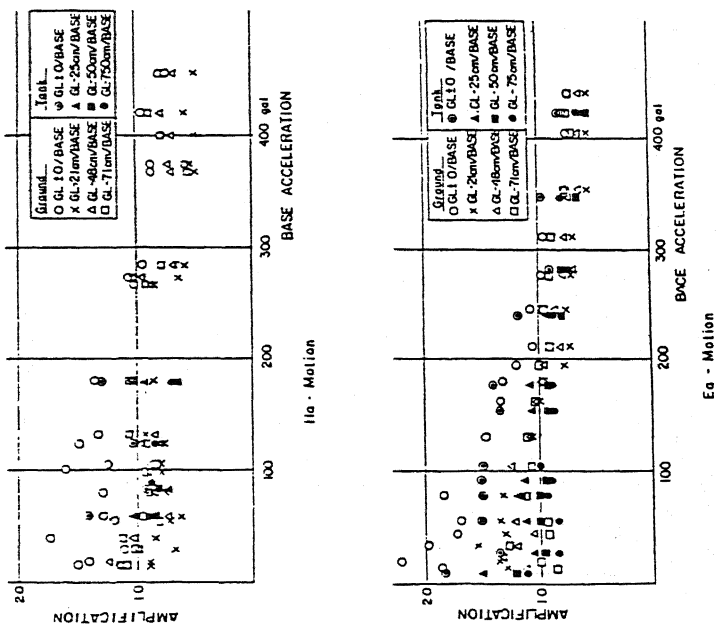


Fig. 4-4 Variation of Amplification with Base Acceleration

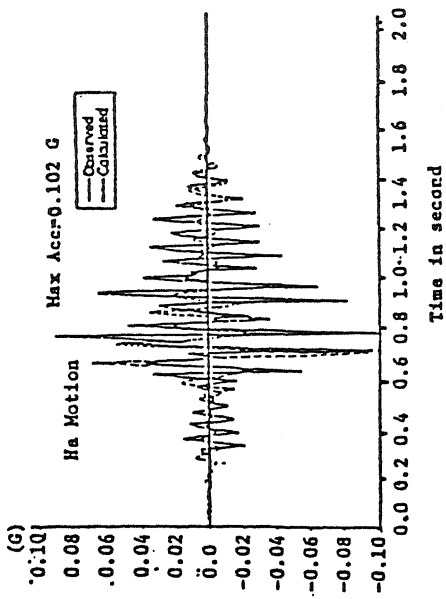


Fig. 6-1 The Longitudinal Distributions of Maximum Acceleration and Stress

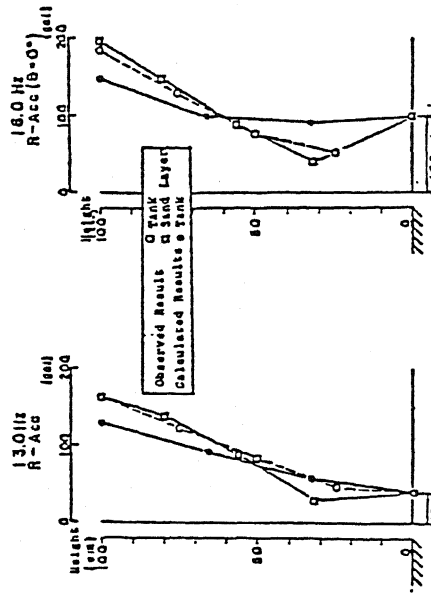


Fig. 6-2 Acceleration Responses of B-Tank

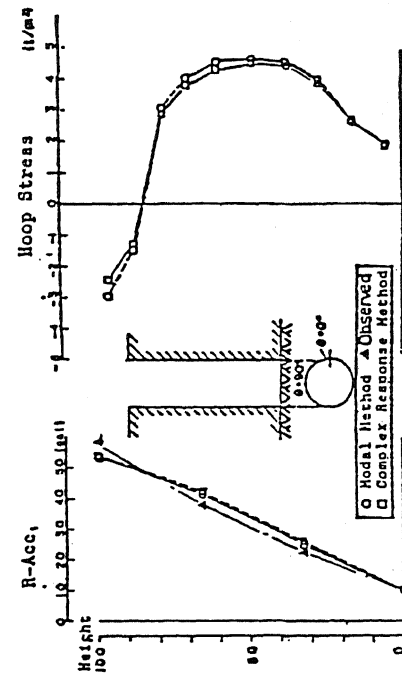


Fig. 6-3 Comparison of Acceleration Time History

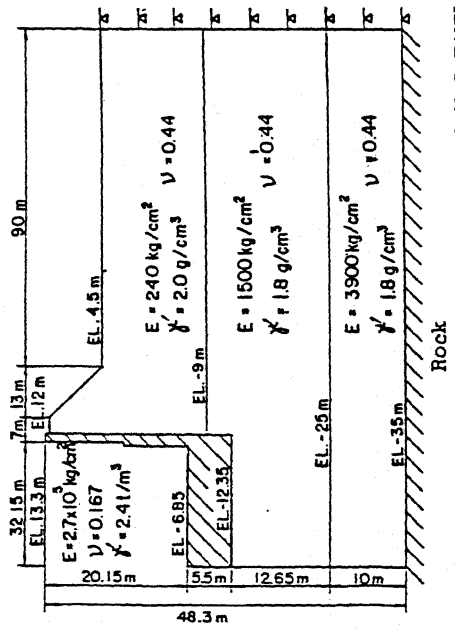


Fig. 7-1 Numerical Model of Actual L.N.G. TANK

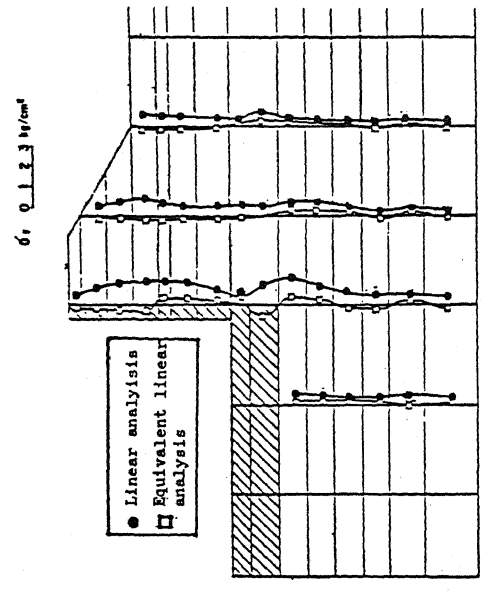


Fig. 7-2 Radial Stress Distributions of The Tank